

Self-Supervised Learning for Multi-Channel Neural Transducer

Atsushi Kojima

Advanced Media, Inc.

a-kojima@advanced-media.co.jp

Abstract

Self-supervised learning, such as with the wav2vec 2.0 framework significantly improves the accuracy of end-to-end automatic speech recognition (ASR). Wav2vec 2.0 has been applied to single-channel end-to-end ASR models. In this work, we explored a self-supervised learning method for a multi-channel end-to-end ASR model based on the wav2vec 2.0 framework. As the multi-channel end-to-end ASR model, we focused on a multi-channel neural transducer. In pre-training, we compared three different methods for feature quantization to train a multi-channel conformer audio encoder: joint quantization, feature-wise quantization and channel-wise quantization. In fine-tuning, we trained the multi-channel conformer-transducer. All experiments were conducted using the far-field in-house and CHiME-4 datasets. The results of the experiments showed that feature-wise quantization was the most effective among the methods. We observed a 66% relative reduction in character error rate compared with the model without any pre-training for the far-field in-house dataset.

Index Terms: Self-supervised learning, wav2vec 2.0, Multi-channel end-to-end speech recognition, Neural transducer, Conformer

1. Introduction

Self-supervised learning significantly improves the accuracy of end-to-end automatic speech recognition (ASR) models such as the attention-based encoder-decoder [1], connectionist temporal classification (CTC) [2] and neural transducers [3]. The most popular framework for self-supervised learning is wav2vec 2.0 [4]. In wav2vec 2.0 pre-training, the model is trained similarly to that in masked language modeling [5]. In fine-tuning, the model is trained using the ASR loss function. Wav2vec 2.0 has been mainly applied to single-channel end-to-end ASR models [4, 6, 7]. In this work, we train a multi-channel end-to-end ASR model based on the wav2vec 2.0 framework.

Multi-channel end-to-end ASR models can improve the robustness of far-field ASR in noisy environments, because the models can capture not only spectral information but also spatial information of the target and interference signals captured from different microphones [8, 9]. In many end-to-end multi-channel ASR architectures [10, 11, 12, 13, 14, 15], a multi-channel neural transducer [14] is promising in terms of efficiency and accuracy.

Multi-channel neural transducers are based on neural transducers such as Transformer-Transducer [16, 17] and Conformer-Transducer [18]. Multi-channel neural transducers can learn the contextual relationship across channels using channel-wise and cross-channel self-attention layers without beamforming [19, 20, 21]. Multi-channel neural transducers outperform typical multi-channel end-to-end ASR models, which are cascaded with neural beamforming [14].

In this work, we train a multi-channel neural transducer based on wav2vec 2.0 pre-training. For training, we explore

three quantization methods: joint quantization, feature-wise quantization and channel-wise quantization. We report the results of experiments using the far-field in-house and public CHiME-4 datasets [9].

In the experiments, we show that feature-wise quantization has the best performance among the quantization methods. We observe 66% and 4.2% relative reductions in character error rate compared with the model without any pre-training for the far-field in-house and CHiME-4 datasets, respectively.

2. Background

2.1. Multi-channel neural transducer

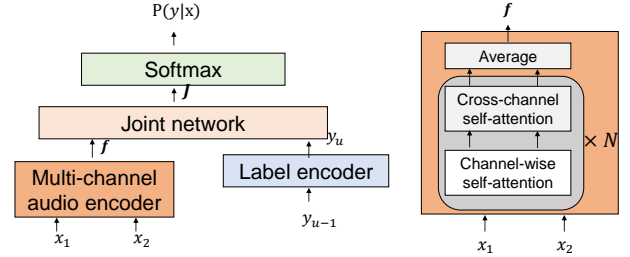


Figure 1: Architecture of multi-channel neural transducer in the case of two channels.

We first describe the architecture of a multi-channel neural transducer. Figure 1 shows an overview of a multi-channel neural transducer in the case of two channels. Given acoustic feature \mathbf{x} and previous tokens \mathbf{y}_{u-1} , the multi-channel audio encoder converts acoustic feature \mathbf{x} to hidden vector \mathbf{f} , and the label encoder predicts a new token \mathbf{y}_u based on past tokens except for a blank token. The joint network outputs vector \mathbf{J} using two hidden vectors from audio and label encoders, and softmax outputs logits.

A multi-channel audio encoder consists of channel-wise self-attention and cross-channel self-attention layers. The channel-wise self-attention layers convert inputs from each channel to hidden vectors independently via multi-head attention (MHA) [22]. The cross-channel self-attention layers learn the contextual relationship across channels. We convert hidden vector h_i of the i th channel from the channel-wise self-attention layers to query Q_i , and the mean vector of the hidden vectors of other channel inputs from the channel-wise self-attention layers is converted to key K_i and value V_i . The MHA is calculated using Q_i , K_i and V_i . Finally, hidden vectors from the cross-channel self-attention layers are fused by taking a simple average. For input features, a multi-channel audio encoder obtains not only amplitude features but also phase features, unlike a single-channel neural transducer.

A multi-channel neural transducer is trained using the recurrent neural network-Transducer (RNN-T) loss [3]. Given

acoustic features \mathbf{x} and label sequence \mathbf{y} , the neural transducer outputs $T \times U$ logits. The RNN-T loss is calculated as the sum of probabilities for all paths using a forward-backward algorithm. The RNN-T loss function is written as

$$\lambda_{\text{RNN-T}} = - \sum_i \log P(\mathbf{y}|\mathbf{x}), \quad (1)$$

$$P(\mathbf{y}|\mathbf{x}) = \sum_{J \in \mathcal{Z}(\mathbf{y}, T)} P(J|\mathbf{x}), \quad (2)$$

where $\mathcal{Z}(\mathbf{y}, T)$ is the set of all alignments of length T for the token sequence.

2.2. Self-supervised learning based on wav2vec 2.0 framework

We next describe self-supervised learning based on the wav2vec 2.0 framework. In wav2vec 2.0 pre-training, the audio encoder is trained by minimizing the contrastive loss. Given target quantized feature \mathbf{q}_t and K distractors (non-target quantized features), the model must identify the true quantized feature among $K + 1$ quantized features $\tilde{\mathbf{q}} \in \mathbf{Q}_t$. The contrastive loss is calculated as

$$\lambda = - \log \frac{\exp(\text{sim}(\mathbf{f}_t, \mathbf{q}_t))}{\sum_{\tilde{\mathbf{q}} \in \mathbf{Q}_t} \exp(\text{sim}(\mathbf{f}_t, \tilde{\mathbf{q}}))}, \quad (3)$$

where \mathbf{f} denotes hidden vectors from the masked audio encoder and sim is a function for calculating the cosine similarity between two vectors: $\text{sim}(\mathbf{a}, \mathbf{b}) = \mathbf{a}^T \mathbf{b} / \|\mathbf{a}\| \|\mathbf{b}\|$.

An audio encoder consists of Transformer [22] or Conformer [18]. A quantizer consists of a quantization [4] or linear [6] layer.

3. Self-supervised learning for multi-channel neural transducer

For the training of the multi-channel audio encoder, we explore three quantization methods: joint quantization, feature-wise quantization and channel-wise quantization.

3.1. Joint quantization

Figure 2 shows joint quantization. In this figure, $X^{\text{amplitude}}$ and X^{phase} are the amplitude and phase features, respectively. \mathbf{f} and \mathbf{q} are the hidden vector from the masked features and the quantized feature as in figure, respectively. This example shows the case of two channels. In this approach, the quantizer converts concatenated vectors $[X_1^{\text{amplitude}}, X_2^{\text{amplitude}}, X_2^{\text{amplitude}}, X_2^{\text{phase}}]$ to quantized vector \mathbf{q} . The quantizer consists of a single linear layer.

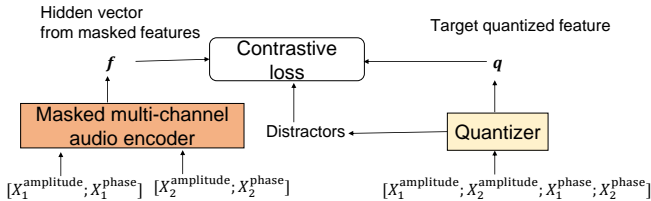


Figure 2: Joint quantization in the case of two channels.

3.2. Feature-wise quantization

Figure 3 shows feature-wise quantization in the case of two channels. In this method, the quantization module consists of amplitude, phase and joint quantizers. The amplitude quantizer converts amplitude features $[X_1^{\text{amplitude}}, X_2^{\text{amplitude}}]$ to quantized amplitude features $\mathbf{q}^{\text{amplitude}}$. The phase quantizer converts phase features $[X_1^{\text{phase}}, X_2^{\text{phase}}]$ to quantized phase features $\mathbf{q}^{\text{phase}}$. The joint quantizer obtains the two vectors $[\mathbf{q}^{\text{amplitude}}, \mathbf{q}^{\text{phase}}]$ from the two quantizers and converts them to quantized feature \mathbf{q} . All quantizers consist of linear layers.

3.3. Channel-wise quantization

Figure 4 shows channel-wise quantization. In this method, the quantization module consists of channel quantizers, the attention and the joint quantizer. The channel quantizers convert the amplitude and phase features $[X_c^{\text{amplitude}}, X_c^{\text{phase}}]$ from each input channel to channel-wise quantized features \mathbf{q}_c . To capture the contextual relationship across channels, the attention was calculated. For instance, the attention for the first channel in the case of two channels is calculated as

$$\mathbf{a}_1 = \text{Softmax}(\mathbf{w}^T \text{Tanh}(U X_1 + H X_2 + \mathbf{b})), \quad (4)$$

where $X_1 = [X_1^{\text{amplitude}}, X_1^{\text{phase}}]$, $X_2 = [X_2^{\text{amplitude}}, X_2^{\text{phase}}]$ and \mathbf{w} , U , H and \mathbf{b} are model parameters. The attention is used to calculate weighted quantized vector \mathbf{q}_c' . The joint quantizer converts the weighted quantized features from each channel quantizer to quantized vector \mathbf{q} .

4. Experiments

4.1. Data preparation

Far-field in-house dataset As the experimental dataset, we use the far-field in-house dataset, which consists of 104.3 hours of transcribed Japanese speech. The speech is recorded by a two-channel linear microphone array with an inter-microphone spacing of 8 mm. The amounts of training and test data are 102 and 2.3 hours, respectively. For pre-training and fine-tuning, we use the training set, and for the evaluation, we use the test set. For this dataset, we report the character error rate (CER).

CHiME-4 dataset We also use the CHiME-4 dataset to evaluate our proposed method. Speech in English is recorded by six microphones. For efficient training, we pick up the first and sixth microphone channels as input signals. In this experiment, we use training and evaluation sets on real data. For pre-training and fine-tuning, we use the training set. For evaluation, we use the eval set. For this dataset, we report the word error rate (WER) and CER.

4.2. Model details

We next describe the architecture of the multi-channel neural transducer. We use eight conformer layers and a unidirectional long short-term memory (LSTM) layer with 256 hidden nodes for the multi-channel audio and label encoders, respectively. Table 1 shows the parameters of the Conformer [18] encoder model. The parameter size of the multi-channel audio encoder is 15.0 (M). The joint network obtains 512-dimensional vectors from audio and label encoders, and outputs 256-dimensional vector with Tanh activation. Finally, softmax outputs logits.

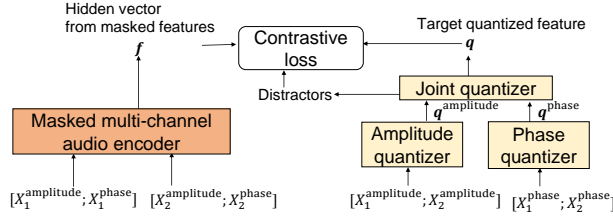


Figure 3: Feature-wise quantization.

Table 1: Multi-channel Conformer encoder architecture.

Parameter	Value
Number of layers	8
Number of channels	2
Number of heads	8
Head dimension	32
Kernel size	7
Number of hidden nodes	256
Position-wise feed-forward dimension	512

For the amplitude feature, we use the log-STFT square magnitude. For the phase feature, we use cosine interchannel phase differences (cosIPD) and sinIPD [23]. The features are extracted every 10 ms with a window size of 25 ms from audio samples. We set the FFT size as 512.

In the wav2vec 2.0 pre-training, we train the multi-channel audio encoder by minimizing the contrastive loss. We mask 50% of the time steps and set the number of distractors as 100. The distractors are uniformly sampled from other masked time steps of the same utterance.

For fine-tuning, we train the multi-channel neural transducer by minimizing the RNN-T loss. As the baseline system, we use the multi-channel neural transducer without any pre-training. For the far-field in-house dataset, the model outputs 715 characters and a blank token. For the CHiME-4 dataset, the model outputs 26 lower-case alphabet characters, three special tokens (apostrophe, period and whitespace) and a blank token. In addition, gradient clipping is applied with a value of 5 to avoid an exploding gradient. We apply SpecAugment [24] to improve robustness. For the training of all models, we use the Transformer learning schedule [22]. We also use the Adam optimizer [25], setting $\beta_1 = 0.9$, $\beta_2 = 0.98$ and $\epsilon = 10$. All networks are implemented using Pytorch [26].

4.3. Results

4.3.1. Far-field in-house dataset

Table 2 shows the results of feature-wise quantization for the far-field in-house dataset. In this experiment, we investigate the effect of the activation function for the amplitude and phase quantizers. Compared with the result of the model without any pre-training (exp0), we observe an improvement for all pre-training methods (exp1, exp2, exp3, exp4). In addition, the amount of improvement depends on the activation function (exp1, exp2, exp4). We observe a 66% relative reduction in CER using the quantization method employing the amplitude

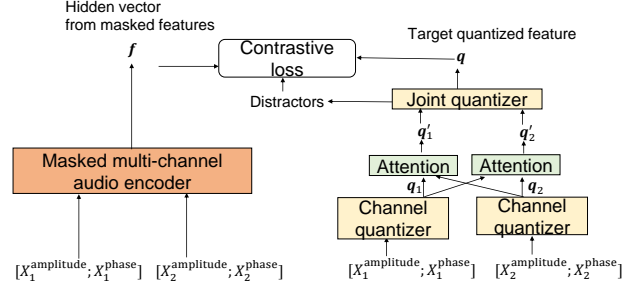


Figure 4: Channel-wise quantization.

Table 2: Results of feature-wise quantization for far-field in-house dataset. Results are given as relative character error rate reduction (CERR) [%]. A positive value indicates an improvement.

ID	pre-training	quantization	amplitude quantizer activation	phase quantizer activation	CERR (%)
exp0	-	-	-	-	0
exp1	✓	feature	Swish	Swish	58.1
exp2	✓	feature	Swish	ReLU	60.5
exp3	✓	joint	-	-	62.1
exp4	✓	feature	Swish	None	66

quantizer with Swish activation [27] and the phase quantizer without any activation (exp4). The CER of the method was lower than that for joint quantization (exp3).

Table 3: Results of channel-wise quantization for far-field in-house dataset. Results are given as relative character error rate reduction (CERR) [%]. A positive value indicates an improvement.

ID	pre-training	quantization	CERR (%)
exp0	-	-	0
exp3	✓	joint	62.1
exp5	✓	channel	49.1

Table 3 shows the results of channel-wise quantization. Compared with the result of the model without any pre-training (exp0), the quantization method also reduced CER (exp5). The improvement was greater for joint quantization (exp3) than for channel-wise quantization (exp5).

4.3.2. CHiME-4 dataset

Table 4 shows the results of feature-wise quantization for the CHiME-4 dataset. Compared with the result of the model without any pre-training (expA), we observe an improvement for all pre-training methods (expB, expC, expD, expE), the same as that for the far-field in-house dataset. We observe a 2.4% relative reduction in WER using the quantization method employing the amplitude quantizer with Swish activation and the phase quantizer with Swish activation (expB). We observe a 4.2% relative reduction in CER using the quantization method employing the amplitude quantizer with Swish activation and the phase quantizer without any activation (expE). Compar-

ing the improvement of CER the for far-field in-house dataset, the improvement of CER for the CHiME-4 dataset was small. We concluded that this is caused by the amount of training data in the CHiME-4 dataset being smaller than that in the far-field in-house dataset.

Table 4: *Results of feature-wise quantization for CHiME-4 dataset. Results are given as relative character error rate reduction (CERR) [%] and relative word error rate reduction (WERR) [%]. A positive value indicates an improvement.*

ID	pre-training	quantization	amplitude quantizer activation	phase quantizer activation	CERR (%)	WERR (%)
expA	-	-	-	-	0	0
expB	✓	feature	Swish	Swish	3.6	2.4
expC	✓	feature	Swish	ReLU	2.6	1.7
expD	✓	joint	-	-	3.2	1.4
expE	✓	feature	Swish	None	4.2	0.1

4.4. Analysis of hidden vectors

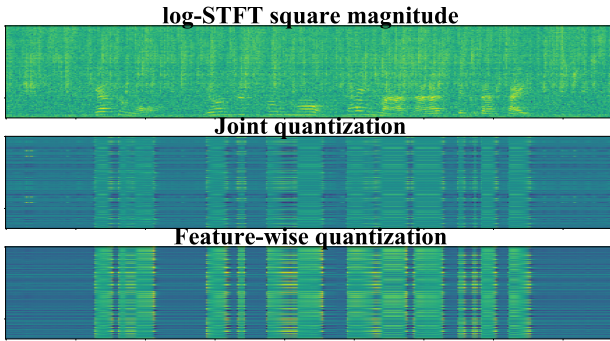


Figure 5: *Analysis of hidden vectors after self-supervised learning.*

We next analyze the hidden vectors from the multi-channel audio encoder after pre-training. Figure 5 shows hidden vectors from multi-channel audio encoders trained by different quantization methods for the far-field in-house dataset. The upper figure shows the log-STFT square magnitude. The middle figure shows the hidden vector from the multi-channel audio encoder trained by joint quantization (exp3). The lower figure shows the hidden vector from the multi-channel audio encoder trained by feature-wise quantization (exp4). By comparing the hidden vectors, we observe a clearer contrast between the speech and noise sections for feature-wise quantization. This result suggests that the multi-channel audio encoder trained by feature-wise quantization learns the latent representation better than the multi-channel audio encoder trained by joint quantization in terms of noise robustness.

5. Conclusion

In this work, we trained a multi-channel neural transducer based on wav2vec 2.0 pre-training. For the training, we explored three quantization methods: joint quantization, feature-wise quantization and channel-wise quantization. We reported the results of experiments using the far-field in-house and public datasets. We experimentally showed that the feature-wise quantization method had the best performance. We observed 66% and 4.2%

relative reductions in CER compared with the model without any pre-training for the far-field in-house and CHiME-4 datasets, respectively.

6. References

- [1] W. Chan, N. Jaitly, Q. Le and O. Vinyals, “Listen, attend and spell: A neural network for large vocabulary conversational speech recognition,” in *Proc. ICASSP*, 2016.
- [2] A. Graves, S. Fernández, F. Gomez and J. Schmidhuber, “Connectionist temporal classification: Labelling unsegmented sequence data with recurrent neural networks,” in *Proc. ICML*, 2006.
- [3] A. Graves, “Sequence transduction with recurrent neural networks,” *arXiv preprint arXiv:1211.3711*, 2012.
- [4] A. Baevski, H. Zhou, A. Mohamed and M. Auli, “wav2vec 2.0: A framework for self-supervised learning of speech representations,” *arXiv preprint arXiv:2006.11477*, 2020.
- [5] J. Devlin, M.-W. Chang, K. Lee and K. Toutanova, “Bert: Pre-training of deep bidirectional transformers for language understanding,” *arXiv, abs/1810.04805*, 2018.
- [6] Y. Zhang, J. Qin, D. S. Park, W. Han, C.-C. Chiu, R. Pang, Q. V. Le and Y. Wu, “Pushing the limits of semi-supervised learning for automatic speech recognition,” *arXiv preprint arXiv:2010.10504*, 2020.
- [7] S. Sadhu, D. He, C.-W. Huang, S. H. Mallidi, M. Wu, A. Rastrow, A. Stolcke, J. Droppo and R. Maas, “Wav2vec-C: A self-supervised model for speech representation learning,” in *Proc. INTERSPEECH*, 2021.
- [8] R. Haeb-Umbach, J. Heymann, L. Drude, S. Watanabe, M. Delcroix and T. Nakatani, “Far-field automatic speech recognition,” *Proc. IEEE*, 2020.
- [9] E. Vincent, S. Watanabe, A. A. Nugraha, J. Barker and R. Marxer, “An analysis of environment, microphone and data simulation mismatches in robust speech recognition,” *Computer Speech & Language*, vol. 46, pp. 535-557, 2017.
- [10] T. Ochiai, S. Watanabe, T. Hori and J. R. Hershey, “Multichannel end-to-end speech recognition,” *arXiv preprint arXiv:1703.04783*, 2017.
- [11] X. Chang, W. Zhang, Y. Qian, J. Le Roux and S. Watanabe, “MIMO-SPEECH: End-to-end multi-channel multi-speaker speech recognition,” in *Proc. ASRU*, 2019.
- [12] A. S. Subramanian, X. Wang, S. Watanabe, T. Taniguchi, D. Tran and Y. Fujita, “An investigation of end-to-end multichannel speech recognition for reverberant and mismatch conditions,” *arXiv preprint arXiv:1904.09049*, 2019.
- [13] F. Chang, M. Radfar, A. Mouchtaris, B. King and S. Kunzmann, “End-to-end multi-channel Transformer for speech recognition,” in *Proc. ICASSP*, 2021.
- [14] F. Chang, M. Radfar, A. Mouchtaris and M. Omologo, “Multi-channel Transformer Transducer for speech recognition,” in *Proc. INTERSPEECH*, 2021.
- [15] B. Li, T. N. Sainath, R. J. Weiss, K. W. Wilson and M. Bacchiani, “Neural network adaptive beamforming for robust multichannel speech recognition,” in *Proc. INTERSPEECH*, 2016.
- [16] C. F. Yeh, J. Mahadeokar, K. Kalgaonkar, Y. Wang, D. Le, M. Jain, K. Schubert, C. Fuegen and M. L. Seltzer, “Transformer-Transducer: End-to-end speech recognition with self-attention,” in *Proc. INTERSPEECH*, 2020.
- [17] Q. Zhang, H. Lu, H. Sak, A. Tripathi, E. McDermott, S. Koo and S. Kumar, “Transformer Transducer: A streamable speech recognition model with Transformer encoders and RNN-T loss,” in *Proc. INTERSPEECH*, 2020.
- [18] A. Gulati, J. Qin, C.-C. Chiu, N. Parmar, Y. Zhang, J. Yu, W. Han, S. Wang, Z. Zhang, Y. Wu and R. Pang, “Conformer: Convolution-augmented transformer for speech recognition,” in *Proc. INTERSPEECH*, 2020.

- [19] J. Heymann, L. Drude and R. Haeb-Umbach, "Neural network based spectral mask estimation for acoustic beamforming," in *Proc. ICASSP*, 2016.
- [20] H. Erdogan, J. Hershey, S. Watanabe, M. Mandel, and J. Le Roux, "Improved MVDR beamforming using single-channel mask prediction networks," in *Proc. INTERSPEECH*, 2016.
- [21] T. Higuchi, K. Kinoshita, N. Ito, S. Karita and T. Nakatani, "Frame-by-frame closed-form update for mask-based adaptive MVDR beamforming," in *Proc. ICASSP*, 2018.
- [22] A. Vaswani, N. Shazeer, N. Parmar, J. Uszkoreit, L. Jones, A. N. Gomez, L. Kaiser and I. Polosukhin, "Attention is all you need," in *Proc. NIPS*, 2017.
- [23] Z. Wang, J. Le Roux and J. R. Hershey, "Multi-channel deep clustering: Discriminative spectral and spatial embeddings for speaker-independent speech separation," in *Proc. ICASSP*, 2018.
- [24] D. S. Park, W. Chan, Y. Zhang, C. Chiu, B. Zoph, E. D. Cubuk and Q. V. Le, "SpecAugment: A simple data augmentation method for automatic speech recognition," in *Proc. INTERSPEECH*, 2019.
- [25] D. P. Kingma and J. Ba, "Adam: A method for stochastic optimization," in *Proc. ICLR*, 2015.
- [26] A. Paszke, S. Gross, F. Massa, A. Lerer, J. Bradbury, G. Chanan, T. Killeen, Z. Lin, N. Gimelshein, L. Antiga, A. Desmaison, A. Köpf, E. Yang, Z. DeVito, M. Raison, A. Tejani, S. Chilamkurthy, B. Steiner, L. Fang, J. Bai and S. Chintala, "PyTorch: An imperative style, high-performance deep learning library," in *Proc. NeurIPS*, 2019.
- [27] P. Ramachandran, B. Zoph and Q. V Le, "Searching for activation functions," *arXiv preprint arXiv:1710.05941*, 2017.